Growth differentiation factor 9:bone morphogenetic protein 15 heterodimers are potent regulators of ovarian functions

Jia Peng[a,b], Qinglei Li[c], Karen Wigglesworth[d], Adithya Rangarajan[e], Chandramohan Kattamuri[f], Randall T. Peterson[g], John J. Eppig[d], Thomas B. Thompson[f], and Martin M. Matzuk[a,b,e,h,i,j,1]

Departments of [a]Pathology and Immunology, [b]Molecular and Human Genetics, [e]Molecular and Cellular Biology, and [h]Pharmacology, [i]Center for Drug Discovery, and [j]Center for Reproductive Medicine, Baylor College of Medicine, Houston, TX 77030; [c]Department of Veterinary Integrative Biosciences, Texas A&M University, College Station, TX 77843; [d]The Jackson Laboratory, Bar Harbor, ME 04609; [f]Department of Molecular Genetics, Biochemistry and Microbiology, University of Cincinnati, Cincinnati, OH 45221; [g]Cardiovascular Research Center, Massachusetts General Hospital and Harvard Medical School, Boston, MA 02114

The TGF-β superfamily is the largest family of secreted proteins in mammals, and members of the TGF-β family are involved in most developmental and physiological processes. Growth differentiation factor 9 (GDF9) and bone morphogenetic protein 15 (BMP15), oocyte-secreted paralogs of the TGF-β superfamily, have been shown genetically to control ovarian physiology. Although previous studies found that GDF9 and BMP15 homodimers can modulate ovarian pathways in vitro, the functional species-specific significance of GDF9:BMP15 heterodimers remained unresolved. Therefore, we engineered and produced purified recombinant mouse and human GDF9 and BMP15 homodimers and GDF9:BMP15 heterodimers to compare their molecular characteristics and physiological functions. In mouse granulosa cell and cumulus cell expansion assays, mouse GDF9 and human BMP15 homodimers can up-regulate cumulus expansion-related genes (*Ptx3*, *Has2*, and *Ptgs2*) and promote cumulus expansion in vitro, whereas mouse BMP15 and human GDF9 homodimers are essentially inactive. However, we discovered that mouse GDF9:BMP15 heterodimer is ~10- to 30-fold more biopotent than mouse GDF9 homodimer, and human GDF9:BMP15 heterodimer is ~1,000- to 3,000-fold more bioactive than human BMP15 homodimer. We also demonstrate that the heterodimers require the kinase activities of ALK4/5/7 and BMPR2 to activate SMAD2/3 but unexpectedly need ALK6 as a coreceptor in the signaling complex in granulosa cells. Our findings that GDF9:BMP15 heterodimers are the most bioactive ligands in mice and humans compared with homodimers explain many puzzling genetic and physiological data generated during the last two decades and have important implications for improving female fertility in mammals.

female reproduction | in vitro maturation | TGF-β signaling

Ligands of the TGF-β superfamily, the largest family of secreted proteins in mammals, are synthesized as dimers and bind transmembrane type 1 and type 2 serine-threonine kinase receptors to activate downstream signaling cascades (e.g., the SMADs) in many developmental, physiological, and pathophysiological processes (1, 2). Growth differentiation factor 9 (GDF9) and bone morphogenic protein 15 (BMP15) are key oocyte-secreted members of the TGF-β superfamily and can regulate female fertility in several mammals (2, 3). Although GDF9 and BMP15 are closely related paralogs, they have been shown in vitro to signal through divergent SMAD2/3 and SMAD1/5/8 pathways, respectively (4–6).

By studying gene knockouts and mutant models, putative roles of GDF9 and BMP15 in female reproduction have been described in mice, sheep, and humans. Our group previously discovered that *Gdf9*-null female mice are sterile (7), and *Gdf9*^{+/−}*Bmp15*^{−/−} double-mutant mice had more severe fertility defects than subfertile *Bmp15*^{−/−} mice (8, 9). *BMP15* or *GDF9* heterozygous mutant sheep have increased litter size, whereas homozygous mutants are sterile and phenocopy *Gdf9*^{−/−} mice (10, 11). In humans,

mutations in *GDF9* and *BMP15* have been associated with premature ovarian failure and dizygotic twinning (12–14). These data suggest synergistic functions of the two gene products and potential species-specific differences in the bioactivity of these proteins. Although an in vitro study has detected the GDF9:BMP15 heterodimer by immunoprecipitation (15), and cooperative effects of the two homodimers were studied by other groups (16–18), the functions of GDF9:BMP15 heterodimers in any species remain largely unknown.

In the present study, we demonstrate that GDF9:BMP15 heterodimers are the most bioactive ligands in the regulation of cumulus expansion genes. These heterodimers signal through a unique BMP receptor type 2 (BMPR2)-ALK4/5/7-ALK6 receptor complex to induce the phosphorylation of SMAD2/3 in human and mouse granulosa cells. Our findings open up prospects for the understanding of the synergistic roles of GDF9 and BMP15 proteins in ovarian functions and have important implications for improving female reproductive productivity in mammals.

Results

Purification of Human and Mouse GDF9:BMP15 Heterodimers and Initial Testing of Their Activities. To reveal possible activities of GDF9:BMP15 heterodimers in mammals, we engineered the

Significance

Although genetic studies have uncovered critical functions of GDF9 and BMP15 in female reproduction, many genetic and physiologic data for these ligands remain perplexing. Here we establish that mouse and human GDF9:BMP15 heterodimers are the most biopotent regulators of ovarian granulosa cell functions. Moreover, GDF9:BMP15 heterodimers require a unique signaling complex that includes the type 2 receptor BMPR2, an ALK4/5/7 type 1 kinase receptor, and an ALK6 type 1 co-receptor. GDF9:BMP15 binding to this complex stimulates phosphorylation of SMAD2/3. Our findings explain intraspecies and interspecies functions of these oocyte-synthesized proteins and have key implications for the regulation of female fertility.

human (h) and mouse (m) GDF9 and BMP15 cDNAs to encode subunit-specific tags (MYC or FLAG) at the N termini of the proteins (Fig. S1*A*). The MYC and FLAG tags were critical for purification and accurate quantification of the proteins. As in our previous study (6), optimized proteolytic cleavage sites for the mouse and human GDF9 and BMP15 precursors were inserted before the epitope tags to facilitate production of the mature proteins. We purified either homodimers (when the subunits were expressed individually in HEK-293T cells) or heterodimers (when both subunits were produced simultaneously in the same cell) (Fig. 1*A*). Western blot analysis was used to detect BMP15 by anti-FLAG and GDF9 by anti-MYC (or anti-GDF9) when both subunits were produced together (Fig. 1*B* and Fig. S1*B*). Immunoprecipitation using anti-FLAG agarose yielded a mixture of BMP15 homodimers (~75%) and GDF9:BMP15 heterodimers (~25%) because of the presence of the FLAG tag in both dimers.

In response to the ovulatory luteinizing hormone surge, cumulus cells become expanded and produce a complex extracellular matrix (ECM), which is essential for ovulation, fertilization, and subsequent embryonic development. This highly coordinated process is known as "cumulus expansion" and requires oocyte-derived paracrine factors (19, 20). Several genes expressed in granulosa cells, including hyaluronan synthase 2 (*Has2*) (21, 22), pentraxin 3 (*Ptx3*) (23), and prostaglandin synthase 2 (*Ptgs2*) (24, 25), have been shown to function in cumulus expansion. To determine whether the mouse and human homodimers and heterodimers were bioactive, we first tested each ligand for its ability to induce *Ptx3*, *Has2*, and *Ptgs2* mRNAs in established mouse granulosa cell assays. The

hBMP15 homodimer slightly stimulates cumulus expansion-related gene expression at a high concentration (100 ng/mL), but the same concentration of hGDF9 homodimer shows no activity compared with the control (not treated with ligand) (Fig. 1 *C*–*E*). Surprisingly, hGDF9:BMP15 induces *Ptx3*, *Has2*, and *Ptgs2* mRNA expression to a greater extent at a 30-fold lower (3 ng/mL) concentration (Fig. 1 *C*–*E*). In addition to the untreated control, we set up another control in which we treated mouse granulosa cells with a combination of hBMP15 and hGDF9 homodimers. The combination of hBMP15 and hGDF9 homodimers at high concentrations did not alter the induction of *Ptx3*, *Has2*, or *Ptgs2* compared with hBMP15 alone (Fig. 1 *C*–*E*). We also performed similar experiments for mouse homodimers and heterodimers (Fig. 1 *F*–*H*). In contrast to human ligands, mGDF9 is a potent regulator of cumulus expansion genes, but mBMP15 is inactive at the same concentration (100 ng/mL). mGDF9:BMP15 heterodimer at a lower concentration (16 ng/mL) and a mixture mGDF9 and mBMP15 homodimers have activity similar to that of mGDF9, although the inductions of *Ptx3*, *Has2*, and *Ptgs2* appeared to have reached maximum saturation with the concentrations of mGDF9 and mGDF9:BMP15 ligands used in this initial study.

h/mGDF9:BMP15 Heterodimers Are More Potent than Homodimers. To quantify the heterodimer activities, we performed dose–response experiments with human and mouse heterodimers in the mouse granulosa cell assays (Fig. 2). Strikingly, 0.03 ng/mL hGDF9:BMP15 has activity comparable to that of 100 ng/mL hBMP15 homodimer in up-regulating the three cumulus expansion-related transcripts, indicating ~3,000-fold increased activity of the hGDF9:
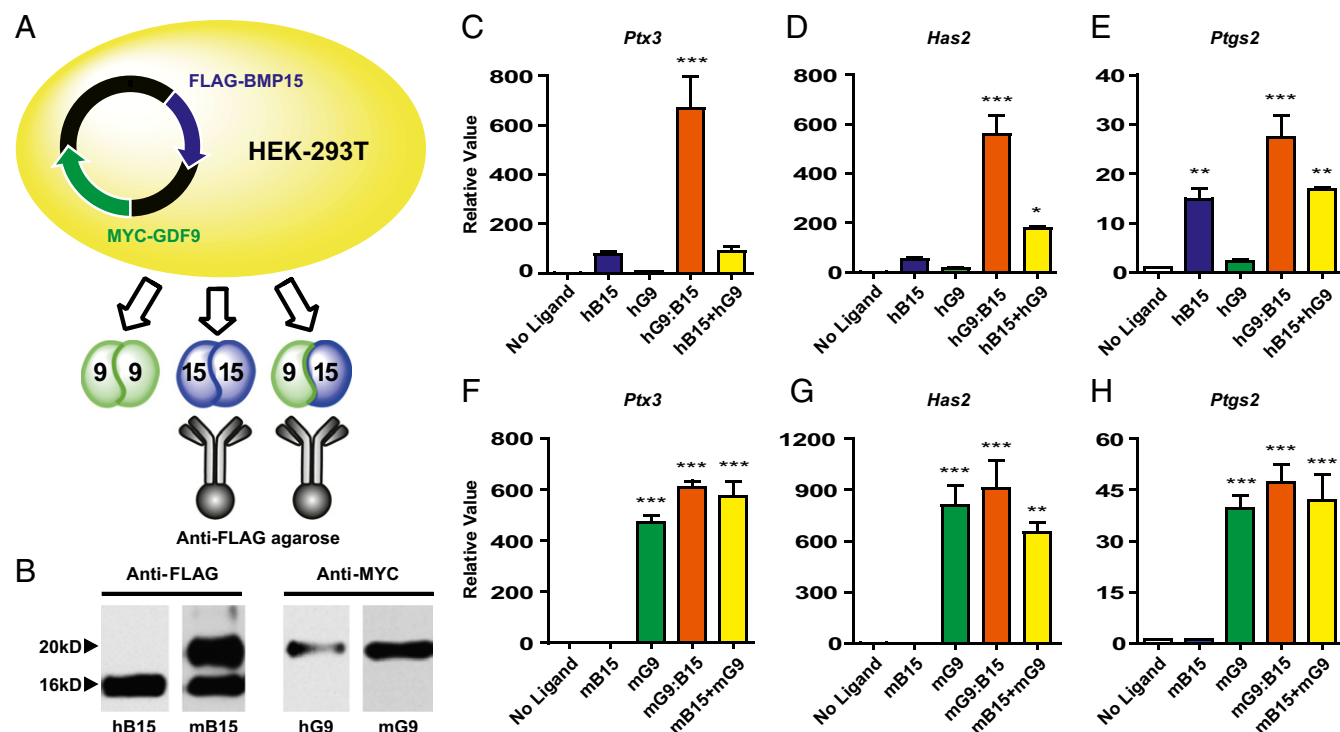
Fig. 1. Purification of h/mGDF9:BMP15 and initial testing of their activities in mouse granulosa cell assay. (*A*) A plasmid containing MYC-tagged GDF9 and FLAG-tagged BMP15 was transfected into HEK-293T cells to yield GDF9 (green), BMP15 (blue), and GDF9:BMP15 (bicolor). Use of anti-FLAG agarose allowed immunoprecipitation of BMP15 and GDF9:BMP15. (*B*) After immunoprecipitation, h/mBMP15 was detected by anti-FLAG, and h/mGDF9 was detected by anti-MYC. (*C*–*H*) Mouse granulosa cells were treated with no ligand (white), 100 ng/mL h/mBMP15 (h/mB15; blue), 100 ng/mL h/mGDF9 (h/mG9; green), 3 ng/mL hGDF9:BMP15 or 16 ng/mL mGDF9:BMP15 (h/mG9:B15; orange), and a mix of 100 ng/mL homodimers (h/mB15+h/mG9; yellow) for 5 h. Total RNA was extracted, and downstream ECM genes *Ptx3* (*C* and *F*), *Has2* (*D* and *G*), and *Ptgs2* (*E* and *H*) were quantified by qPCR and are shown relative to the control (no ligand) sample. Data in *C*–*H* represent the mean ± SEM (*n* = 3). *$P < 0.05$; **$P < 0.01$; ***$P < 0.001$ compared with controls not treated with ligand. (*C*–*E*) Induction of *Ptx3*, *Has2*, or *Ptgs2* with hBMP15 versus combination treatment was not statistically significant. (*F*–*H*) Induction of *Ptx3*, *Has2*, or *Ptgs2* with mGDF9 versus combination treatment was not statistically significant.
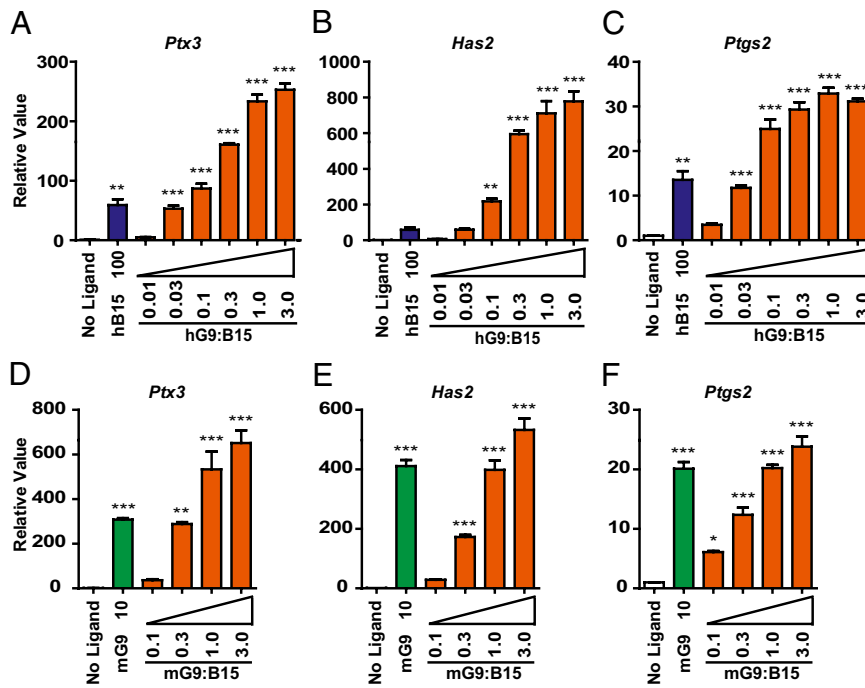
Peng et al.

Fig. 2. h/mGDF9:BMP15 dose-dependent effects in downstream ECM gene regulation. Mouse granulosa cells were treated with serial dilutions of hGDF9: BMP15 (0.01, 0.03, 0.1, 0.3, 1.0, and 3.0 ng/mL) or mGDF9:BMP15 (0.1, 0.3, 1.0, and 3.0 ng/mL). hBMP15 (100 ng/mL) or mGDF9 (10 ng/mL) was used as a positive control. Gene expression of *Ptx3* (*A* and *D*), *Has2* (*B* and *E*), and *Ptgs2* (*C* and *F*) was measured to quantify ligand activities. Data represent the mean ± SEM (*n* = 3). *P < 0.05; **P < 0.01; ***P < 0.001 compared with controls not treated with ligand.

BMP15 heterodimer compared with the hBMP15 homodimer (Fig. 2 *A–C*). In a parallel experiment for mouse ligands, mGDF9: BMP15 is ~10- to 30-fold more biopotent than mGDF9 homodimer (Fig. 2 *D–F*).

Although these results show that GDF9:BMP15 heterodimers are more potent than their homodimers in up-regulating cumulus expansion-related transcripts, we investigated whether heterodimers are sufficient to promote the full process of cumulus expansion in vitro using previously described methods (26). In the presence of epidermal growth factor (EGF), cumulus expansion was induced when mouse oocytectomized (OOX) cumulus cell complexes (i.e., with the resident oocyte microsurgically removed) were treated with one of the four homodimers or with either heterodimer using serial dilutions (Fig. 3 *A–E*). Results of the OOX complex expansion assay matched the results of the previous mouse granulosa cell assay: hGDF9:BMP15 shows about 1,000-fold increased activity compared with hBMP15, whereas mGDF9:BMP15 shows more than 10-fold enhanced biopotency compared with mGDF9 (Fig. 3 *F–G*).

Identification of the h/mGDF9:BMP15 Heterodimer SMAD Signaling Pathway and Type 1 Receptor in Mouse Granulosa Cells. Although GDF9 and BMP15 are closely related paralogs in the TGF-β superfamily, the "active" species-specific homodimers signal via different SMAD pathways: SMAD2/3 for mGDF9 and SMAD1/5 for hBMP15 (4–6). To define the downstream signaling cascades of the heterodimers in mouse granulosa cells, we next examined SMAD1/5/8 and SMAD2/3 phosphorylation levels 1 h after treatment with hBMP15, mGDF9, or GDF9:BMP15 heterodimers (Fig. 4*A*). Compared with the hBMP15 homodimer, the GDF9:BMP15 heterodimers and the mGDF9 homodimer showed minimal SMAD1/5/8 phosphorylation. In contrast, mGDF9:BMP15 and hGDF9: BMP15 dramatically stimulated SMAD2/3 phosphorylation, indicating that SMAD2/3 is the major signaling pathway for GDF9: BMP15 heterodimers. These findings corroborate the importance of the SMAD2/3 pathways in cumulus cell physiology identified

genetically in our laboratory: SMAD2/3 double-knockout mice have severely impaired fertility secondary to defects in cumulus expansion (27), whereas SMAD1/5/8 triple knockouts display minor defects in fertility (28).

A previous in vitro study detected the interaction between BMP15 and the BMP type 1 receptor, ALK6, by coimmunoprecipitation (5). *Alk6*-knockout female mice are sterile because of impaired cumulus expansion (29), suggesting that mGDF9:BMP15 may signal through ALK6 to promote cell expansion. To test if ALK6 is involved in the heterodimer receptor complex, we examined SMAD1/5/8 and SMAD2/3 phosphorylation in *Alk6*$^{-/-}$ mouse granulosa cells after treatment with our ligands (Fig. 4*B*). Because BMP15 is thought to signal through ALK6, phosphorylation of SMAD1/5/8 was reduced in *Alk6*$^{-/-}$ granulosa cells compared with wild-type cells. Furthermore, ALK6 does not appear to play a significant role in GDF9 signaling, because SMAD2/3 signaling was unchanged in the *Alk6*$^{-/-}$ granulosa cells. As anticipated, h/mGDF9:BMP15 heterodimers were unable to phosphorylate SMAD1/5/8 in *Alk6*$^{-/-}$ granulosa cells, but, unexpectedly, SMAD2/3 phosphorylation was abolished. These data indicate that ALK6 is an important type 1 receptor for the heterodimers and is essential in the receptor complex for triggering downstream SMAD2/3 phosphorylation.

To investigate further other type 1 receptor-signaling pathways for the heterodimers, inhibitors specific to particular type 1 receptor subgroups were coincubated with our ligands in the mouse granulosa cell assay (Fig. 4 *C–H*). LDN-193189 (a dorsomorphin derivative) is an inhibitor of ALK2/3/6 (30, 31), and SB-505124 is an inhibitor of ALK4/5/7 (32). Both of these inhibitors function primarily by preventing receptor-regulated SMAD phosphorylation. LDN-193189 significantly decreased hBMP15 activity but showed only a subtle effect on heterodimer action in one of our quantitative PCR (qPCR) assays (Fig. 4 *C–E*). This result indicates that activation of SMAD2/3 by the GDF9:BMP15 heterodimer does not require the kinase activity of ALK6 and also is consistent with the lack of significant SMAD1/5/8 phosphorylation after
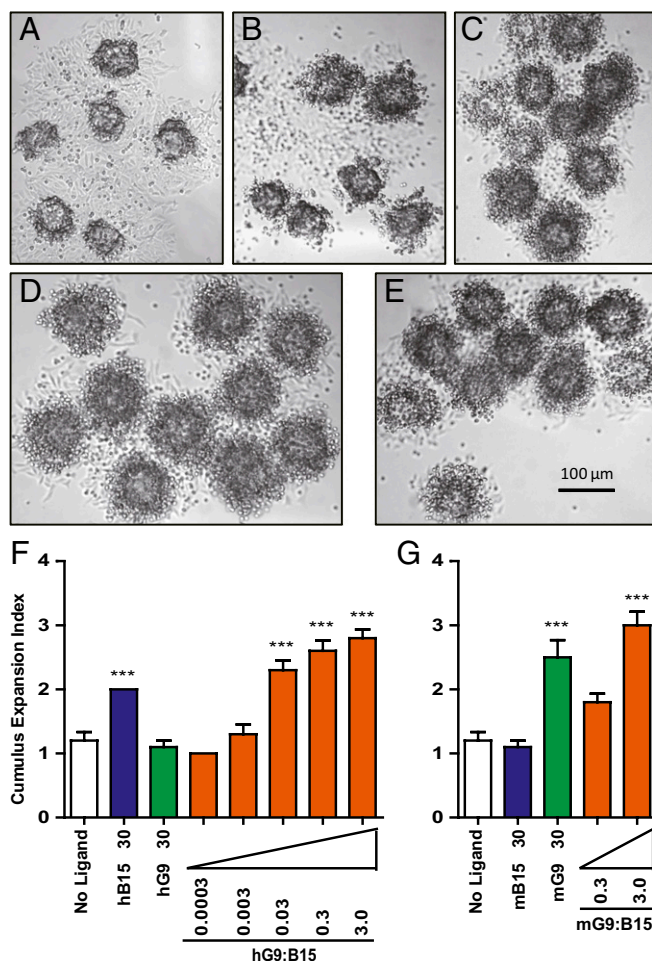
Fig. 3. h/mGDF9:BMP15 dose-dependent effects in OOX cumulus cell expansion. (A–E) Representative photographs of OOX cumulus cells treated with no ligand (A), 30 ng/mL hBMP15 (B), 30 ng/mL mGDF9 (C), 0.3 ng/mL hGDF9:BMP15 (D), or 0.3 ng/mL mGDF9:BMP15 (E) in the presence of EGF (10 ng/mL). (F–G) OOX cumulus cells were treated with 30 ng/mL homodimers and a 1:10 serial dilution of hGDF9:BMP15 (0.0003, 0.003, 0.03, 0.3, and 3.0 ng/mL) or mGDF9:BMP15 (0.3 and 3.0 ng/mL) to test dose-dependent effects in OOX cumulus cell expansion. Data in F and G represent the mean ± SEM (n = 10). ***P < 0.001 compared with controls not treated with ligand.

treatment with the heterodimers (Fig. 4A). In contrast, SB-505124 abolished heterodimer activities, similar to its actions in inhibiting mGDF9 (Fig. 4 F–H). Thus, ALK4/5/7 is the signaling type 1 receptor for GDF9:BMP15 heterodimers and, in combination with a nonsignaling ALK6 receptor, regulates downstream ECM genes.

Identification of the h/mGDF9:BMP15 Heterodimer Type 2 Receptor in Mouse Granulosa Cells. In vitro, BMPR2 is a type 2 receptor for both GDF9 and BMP15 (5, 33). To identify the GDF9:BMP15 heterodimer type 2 receptor, we compared SMAD2/3 phosphorylation levels among treatments with different type 2 receptor extracellular domains (ECDs): BMPR2, ACVR2A, ACVR2B, and TGFBR2 (Fig. 5A and Fig. S2). Only the BMPR2 ECD decreased the activities of mGDF9 and h/mGDF9:BMP15 in SMAD2/3 phosphorylation assays.

To test further the importance of BMPR2 as a heterodimer type 2 receptor in the regulation of cumulus expansion genes, we determined if the BMPR2 ECD could decrease activities of GDF9:BMP15 heterodimers in the mouse granulosa cell assay. We found that BMPR2 ECD attenuated the up-regulation of ECM gene

expression by h/mGDF9:BMP15 heterodimers as well as by hBMP15 and mGDF9 (Fig. 5 B–G).

Confirmation of the SMAD Signaling Pathway by the h/mGDF9:BMP15 Heterodimer in Human Granulosa Cells. To validate our conclusions in human granulosa cells, we tested GDF9:BMP15 heterodimer activities in COV434 cells, an immortalized human granulosa cell line. Similar to the results in mouse granulosa cells, active hBMP15 and mGDF9 homodimers signal via SMAD1/5/8 and SMAD2/3, respectively (Fig. 6A). The h/mGDF9:BMP15 heterodimers use SMAD2/3 as the major signaling pathway (Fig. 6A). Furthermore, assay results in COV434 cells confirmed that the high activity of hGDF9:BMP15 is not the result of a synergistic effect of hGDF9 and hBMP15 homodimers (Fig. 6B).

In dose–response experiments, h/mGDF9:BMP15 heterodimers show dramatically higher activities in SMAD2/3 phosphorylation than their corresponding homodimers (Fig. 6 C and D). We observed SMAD2/3 phosphorylation at the lowest tested dose (0.1 ng/mL) of the hGDF9:BMP15 heterodimer, but there was no apparent SMAD2/3 phosphorylation by the hGDF9 and hBMP15 homodimers when tested at a dose of 100 ng/mL (Fig. 6C). This result confirms the >1,000-fold higher activity of hGDF9:BMP15 compared with hBMP15 that we observed in our mouse granulosa cell assays. When we tested mGDF9 homodimer in the COV434 cells, we observed low phosphorylation of SMAD2/3 at 10 ng/mL of GDF9, approximating the SMAD2/3 phosphorylation by mGDF9: BMP15 heterodimer (0.1–0.3 ng/mL) (Fig. 6D). This result also confirms the ~30-fold higher activity of mGDF9:BMP15 compared with GDF9 that we observed in mouse granulosa cell assays.

Last, we examined the effects of the type 1 inhibitors and type 2 ECDs on the ligand-signaling pathways in COV434 cells. The heterodimer activities in SMAD2/3 phosphorylation assays were abolished specifically by SB-505124 but not by LDN-193189 (Fig. 6 E and F), confirming that ALK4/5/7 is the type 1 receptor kinase that phosphorylates SMAD2/3 in human as well as mouse. To evaluate the GDF9:BMP15 heterodimer type 2 receptor in COV434 cells, we compared SMAD2/3 phosphorylation levels among treatments with four different type 2 receptor ECDs and found that only BMPR2 ECD decreased activities of mGDF9 and hGDF9:BMP15 in SMAD2/3 phosphorylation (Fig. S3).

Discussion

Previous studies have identified a number of heterodimeric TGF-β ligands that have novel functions or enhanced potency compared with the homodimers. For example, inhibins (α:βA and α:βB) antagonize activins (βA:βA, βB:βB, and βA:βB) through their binding to specific and unique receptors (1, 34), and BMP2:BMP7 heterodimers show a specific activity about 20-fold higher than their homodimers in vitro (35). In our studies presented here, we show even more potent bioactivity of recombinant GDF9:BMP15 heterodimers. Based on the results in our paper and the genetic and physiologic findings in mice, rats, sheep, and human, we now present models for the respective activity of homodimers and heterodimers in these species (Fig. 7). In humans, the recombinant GDF9:BMP15 heterodimer was the most bioactive ligand in cumulus expansion in vitro, having more than 1,000-fold greater activity than BMP15 homodimer, whereas GDF9 homodimer was essentially inactive (Fig. 7A). Alternatively, using recombinant mouse dimers, we established that the GDF9:BMP15 heterodimer is ~10- to 30-fold more biopotent than the mGDF9 homodimer, whereas the mBMP15 homodimer is inactive (Fig. 7B). These findings are consistent with the genetic findings in several species. Gdf9-knockout mice are sterile (7) because they lack the ability to synthesize two active dimers (GDF9:BMP15 and GDF9:GDF9). Alternatively, Bmp15-knockout mice are subfertile because they fail to synthesize the most active dimer (GDF9:BMP15) (8). These genetic findings indicate that the continued synthesis of the less active GDF9:GDF9 homodimer partially compensates for hetero-
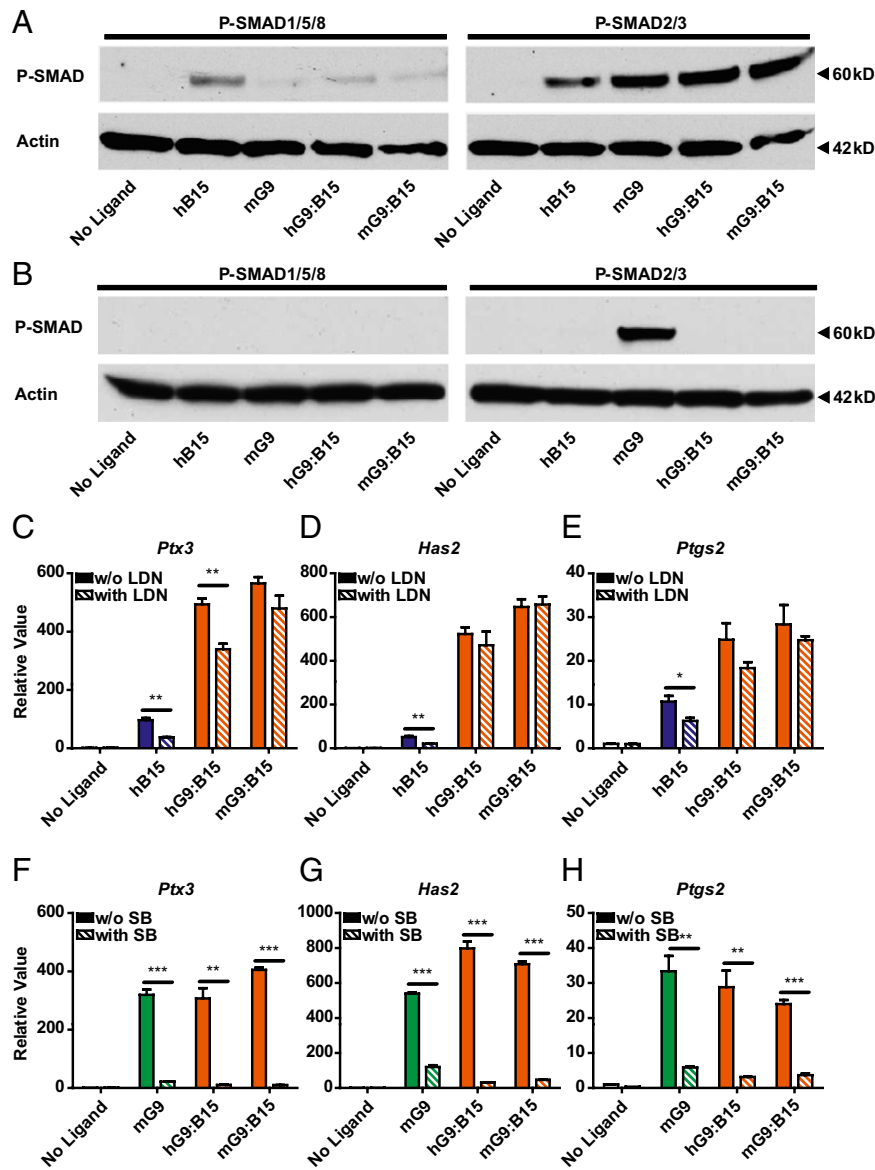
Peng et al.

Fig. 4. Identification of the h/mGDF9:BMP15 SMAD-signaling pathway and type 1 receptors in mouse granulosa cells. (*A*) Wild-type granulosa cells were treated with ligands (100 ng/mL hBMP15, 100 ng/mL mGDF9, 3 ng/mL hGDF9:BMP15, and 16 ng/mL mGDF9:BMP15) for 1 h. Anti–P-SMAD1/5/8 and anti–P-SMAD2/3 were used to detect the two SMAD-signaling pathways. Actin was used as the internal control. (*B*) $Alk6^{-/-}$ granulosa cells were treated with the same ligands to examine the phosphorylation of SMAD1/5/8 and SMAD2/3. Actin was used as the internal control. (*C–H*) The ALK2/3/6 inhibitor LDN-193189 (100 nM) or the ALK4/5/7 inhibitor SB-505124 (1 μM) was coincubated with the ligands to test if the induction of downstream ECM genes *Ptx3* (*C* and *F*), *Has2* (*D* and *G*), and *Ptgs2* (*E* and *H*) was abolished compared with controls not treated with inhibitor. Data in *C–H* represent the mean ± SEM ($n = 3$). *$P < 0.05$; **$P < 0.01$; ***$P < 0.001$.

dimer absence and can cooperate with GDF9:BMP15 heterodimers to regulate granulosa cell function exclusively through the SMAD2/3 pathway (Fig. 7*B*). However, with a further reduction in the production of the GDF9 subunit, $Gdf9^{+/-}Bmp15^{-/-}$ mutant mice show profound fertility defects, and when the mutations are present on a 129 inbred genetic background, these mice are sterile (8).

During evolution, mutations that cause a gene product to become inactive and unnecessary could result eventually in loss of a gene. Thus, the lack of significant activity of mouse BMP15 homodimers or human GDF9 homodimers in granulosa cell assays would suggest that these ligand-encoding genes would disappear during evolution. However, the continued presence of both a *BMP15* gene and a *GDF9* gene in more than 30 evolutionarily diverse mammalian species and other vertebrates sequenced to date suggests that heterodimers are the most active forms within many, if not all, of these

species. Unlike other TGF-β family members such as activin βA, which is nearly 100% conserved in its mature amino acid sequence in almost all mammals, our group previously showed that mouse and human BMP15 mature domains share only 69.6% identity, but mouse and human GDF9 mature domains have 89.6% amino acid identity. Likewise, sheep BMP15 is divergent compared with mouse and human BMP15 (78.9% identity with each), but the mature sequence of sheep GDF9 shows 87.4% and 92.6% identity with mouse and human GDF9, respectively. Coevolutionary divergence in the GDF9 and BMP15 mature coding sequences may have allowed GDF9:BMP15 heterodimers to form, be more active than homodimers, and function as the essential oocyte-secreted TGF-β dimers, especially in women and sheep, and likely in most other mammals.

Previous in vitro studies indicate that the human BMP15 homodimer signals through a complex of BMPR2 (type 2) and ALK6
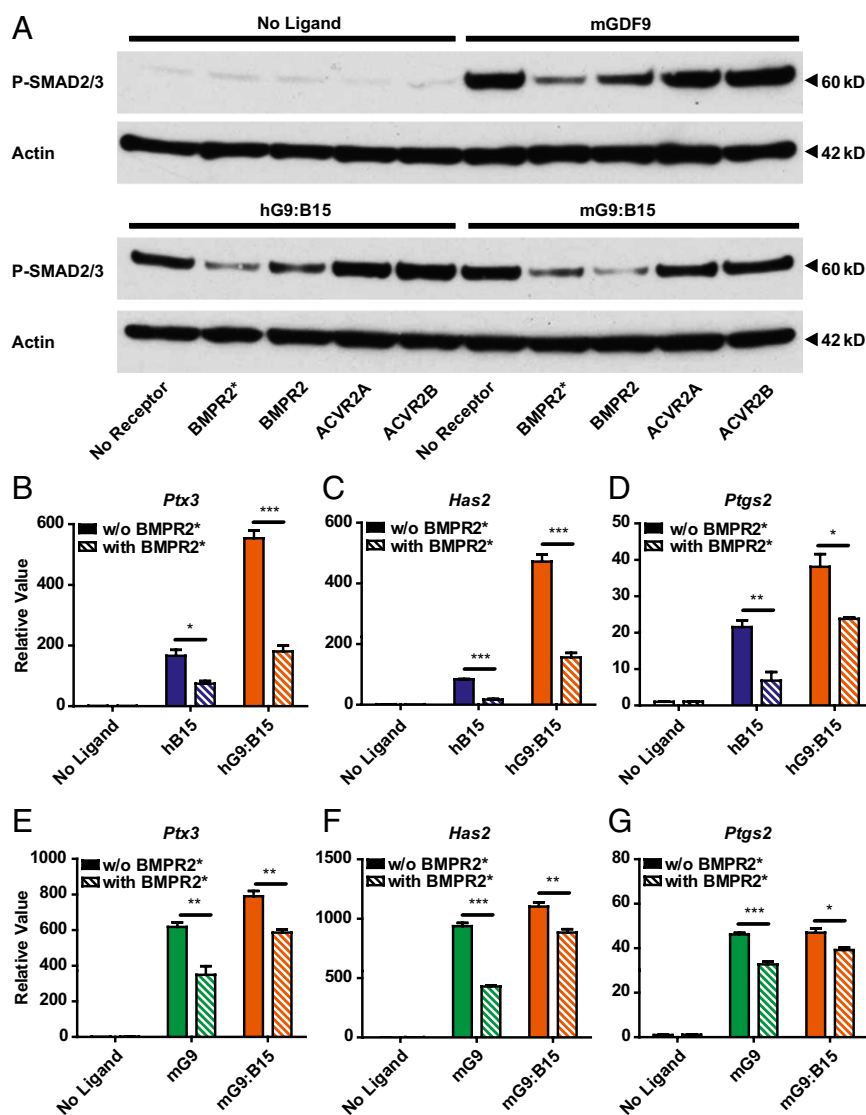
Peng et al.

www.manaraa.com

Fig. 5. Identification of the h/mGDF9:BMP15 type 2 receptor in mouse granulosa cells. (*A*) Ligands (100 ng/mL mGDF9 and 3 ng/mL h/mGDF9:BMP15) were incubated with 1 μg/mL BMPR2* (T.B.T), BMPR2, ACVR2A, or ACVR2B ECD. Anti–P-SMAD2/3 was used to compare SMAD2/3 phosphorylation levels among different type 2 receptor ECD treatments. Actin was used as the internal control. (*B–G*) BMPR2* ECD (1 μg/mL) was incubated with the ligands (100 ng/mL hBMP15, 100 ng/mL mGDF9, 3 ng/mL hGDF9:BMP15, and 16 ng/mL mGDF9:BMP15) to test if the induction of downstream ECM genes *Ptx3* (*B* and *E*), *Has2* (*C* and *F*), and *Ptgs2* (*D* and *G*) was altered compared with controls without the ECD receptor. Data in *B–G* represent the mean ± SEM (n = 3). *P < 0.05; **P < 0.01; ***P < 0.001.

(type 1) (5, 36). Ligand binding to the complex causes BMPR2 to phosphorylate ALK6, which subsequently phosphorylates SMAD1/5/8 to regulate gene expression (Fig. 7*A*). Alternatively, mouse GDF9 homodimers signal through a complex that includes BMPR2 and ALK4/5/7 (Fig. 7*B*). Ligand-induced dimerization of the type 2 and type 1 receptors results in ALK4/5/7 phosphorylation and subsequent phosphorylation of SMAD2/3. Although rat GDF9 homodimers have been reported to signal through ALK5 in an in vitro assay (4), our group discovered that *Alk5* conditional knockout (cKO) mice have no defects in follicular development and cumulus expansion, indicating that ALK5 is not the type 1 receptor through which the GDF9 homodimer signals in the mouse ovary (37). Like BMP15 and GDF9 homodimers, mouse and human GDF9:BMP15 heterodimers signal through BMPR2. Type 1 inhibitor studies indicate that mouse and human GDF9:BMP15 heterodimers require the kinase activity of ALK4/5/7 but do not require kinase signaling from ALK2/3/6. Because GDF9:BMP15 heterodimers are the most active ligands in our granulosa cell assays, and the *Alk5* cKO mice

show normal cumulus expansion (37), unlike *Gdf9*^{+/−}*Bmp15*^{−/−} double-mutant mice (8), we also can exclude ALK5 as the type 1 receptor for the GDF9:BMP15 heterodimer. Furthermore, ALK7 has relatively low expression in the ovary (38). Thus, ALK4 is the most likely type 1 kinase receptor for GDF9:BMP15 heterodimers to phosphorylate SMAD2/3, although this possibility must be tested genetically.

Although the ALK2/3/6 kinase inhibitor LDN-193189 fails to block signaling of mouse and human GDF9:BMP15, the heterodimers fail to signal when ALK6-null granulosa cells are used in our assays. Thus, when the heterodimer binds the complex, BMPR2 (type 2) phosphorylates ALK4 (type 1), and activated ALK4 phosphorylates SMAD2/3 (Fig. 7). Because ALK6 kinase activity is not required for heterodimer signaling, ALK6 must function as a "co-receptor" in the complex. Therefore, our studies reveal that GDF9:BMP15 heterodimers signal through a BMPR2-ALK4/5/7-ALK6 complex. Like other TGF-β–signaling homodimers and heterodimers, the GDF9:BMP15 heterodimeric ligands bind a complex of
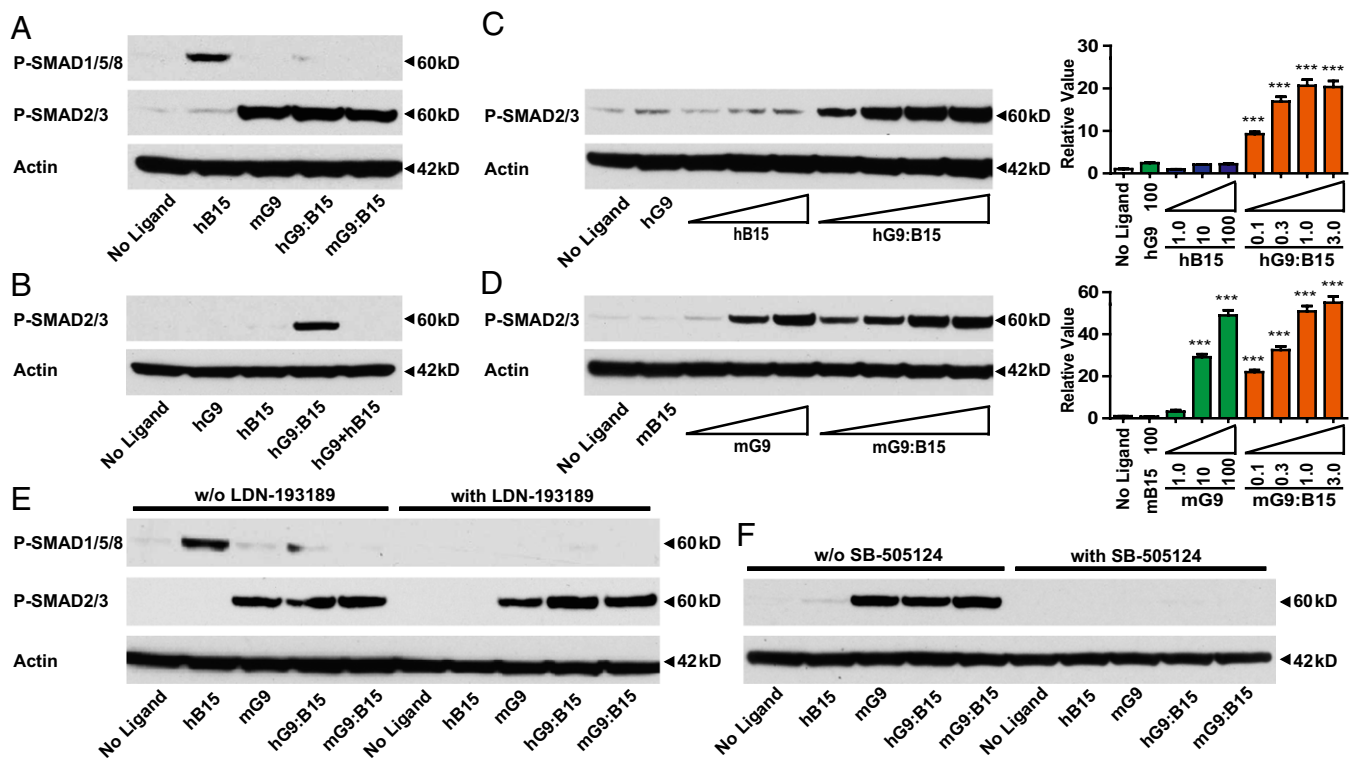
Peng et al.

Fig. 6. Identification of the h/mGDF9:BMP15 SMAD-signaling pathway and type 1 receptors in COV434 cells. (*A*) COV434 cells were treated with 100 ng/mL hBMP15, 100 ng/mL mGDF9, and 3 ng/mL h/mGDF9:BMP15 for 1 h. Anti–P-SMAD1/5/8 and anti–P-SMAD2/3 were used to detect the two P-SMAD–signaling pathways. Actin was used as the internal control. (*B*) COV434 cells were treated with 100 ng/mL hBMP15, 100 ng/mL hGDF9, and 3 ng/mL hGDF9:BMP15 and a mix of their homodimers (100 ng/mL) for 1 h. Anti–P-SMAD2/3 was used to define ligand activities. Actin was used as the internal control. (*C* and *D*) (*Left*) COV434 cells were treated with serial dilutions of hBMP15 or mGDF9 (1.0, 10, or 100 ng/mL) or h/mGDF9:BMP15 (0.1, 0.3, 1.0, or 3.0 ng/mL) to test the dose-dependent effect on SMAD2/3 phosphorylation. Actin was used as the internal control. (*Right*) Western blots of three independent experiments were quantified, and the data are shown as the mean ± SEM (*n* = 10). ***$P < 0.001$ compared with controls not treated with ligand. (*E* and *F*) The ALK2/3/6 inhibitor LDN-193189 (100 nM) or the ALK4/5/7 inhibitor SB-505124 (1 μM) was coincubated with the ligands to test if the induction of SMAD phosphorylation was abolished compared with controls with no inhibitor treatment. Actin was used as the internal control.

two type 2 receptors (in this case BMPR2) and two type 1 receptors [in this case, ALK4 (likely) and ALK6]. Because ALK6 kinase activity is not necessary, it is possible that BMPR2 fails to phosphorylate ALK6, and therefore ALK6 remains in a nonphosphorylated (inactive) state. As reviewed recently (39), heterodimeric members of the BMP subfamily are more potent in vitro and in vivo because (*i*) the heterodimers show higher-affinity binding than homodimers to type 1 and 2 receptors; (*ii*) the ligand:receptor complex is more stable at the cell surface (i.e., is not degraded as quickly); (*iii*) the heterodimers show lower binding to extracellular protein antagonists; and (*iv*) binding of the heterodimeric ligands results in a unique conformation of the receptors including the type 1 receptors. This last point is likely true because we failed to observe SMAD1/5/8 phosphorylation despite the inclusion of ALK6 protein in the complex. Because ALK6 has been shown to have higher affinity for ligands than ALK4, incorporating ALK6 into the receptor complex may provide a mechanism for localizing the GDF9:BMP15 ligand to the cell surface and thereby stabilizing the signaling complex. Because a variety of TGF-β dimers (i.e., activins, inhibins, and BMPs) are expressed throughout ovarian folliculogenesis in all mammals and use similar combinations of these signaling receptors (1, 2), a significant ligand–receptor competition exists in vivo. Therefore, the heightened activity of the heterodimers and unique combination of type 1 and type 2 receptors could result in increased spatiotemporal signaling specificity of the oocyte-secreted heterodimers in the ovaries of women and ewes.

Relative to the activity of GDF9:BMP15 heterodimers, why do mice (and rat) GDF9 homodimers have significant activity (22,

40) compared with human (and sheep) homodimers? In mice, *Gdf9* and *Bmp15* share similar expression patterns: They have low levels of expression in oocytes of primary follicles and increase in oocytes of growing follicles through ovulation (22, 41). Similarly, in the rat GDF9 and BMP15 are expressed in oocytes beginning at the early primary follicle (40, 42). However, although *Gdf9*-null mice are infertile because folliculogenesis is blocked at the primary follicle stage (7), *Alk6*-null females are infertile because of defects in cumulus expansion (29). Furthermore, *Alk6* is expressed in mouse and rat granulosa cells beginning at the secondary (two-layer; type 4) follicle stage (29, 42). These studies and our data suggest that only GDF9 homodimers are required for signaling at the primary follicle stage in mice and rat and indicate that in rodents GDF9:BMP15 heterodimers play a major role in cumulus expansion and ovulation at the preovulatory stage when ALK6 is present (Fig. 7*B*). In contrast, ALK6 is expressed in sheep granulosa cells beginning at the primordial (type 2) follicle stage (17), and mutations in both GDF9 and BMP15 cause a similar block at the primary follicle stage (10, 11). Thus, in sheep, we predict that the activity of the homodimers is somewhat irrelevant, because ALK6 is expressed and GDF9:BMP15 heterodimers are expected to be potent, as in humans (Fig. 7*A*). Unfortunately, we have been unable to identify GDF9:BMP15 heterodimers from either mouse ovary or human follicular fluid because of the lack of high-affinity antibodies to mouse BMP15 and the low levels of these oocyte-secreted proteins (either homodimers or heterodimers) in follicular fluid.
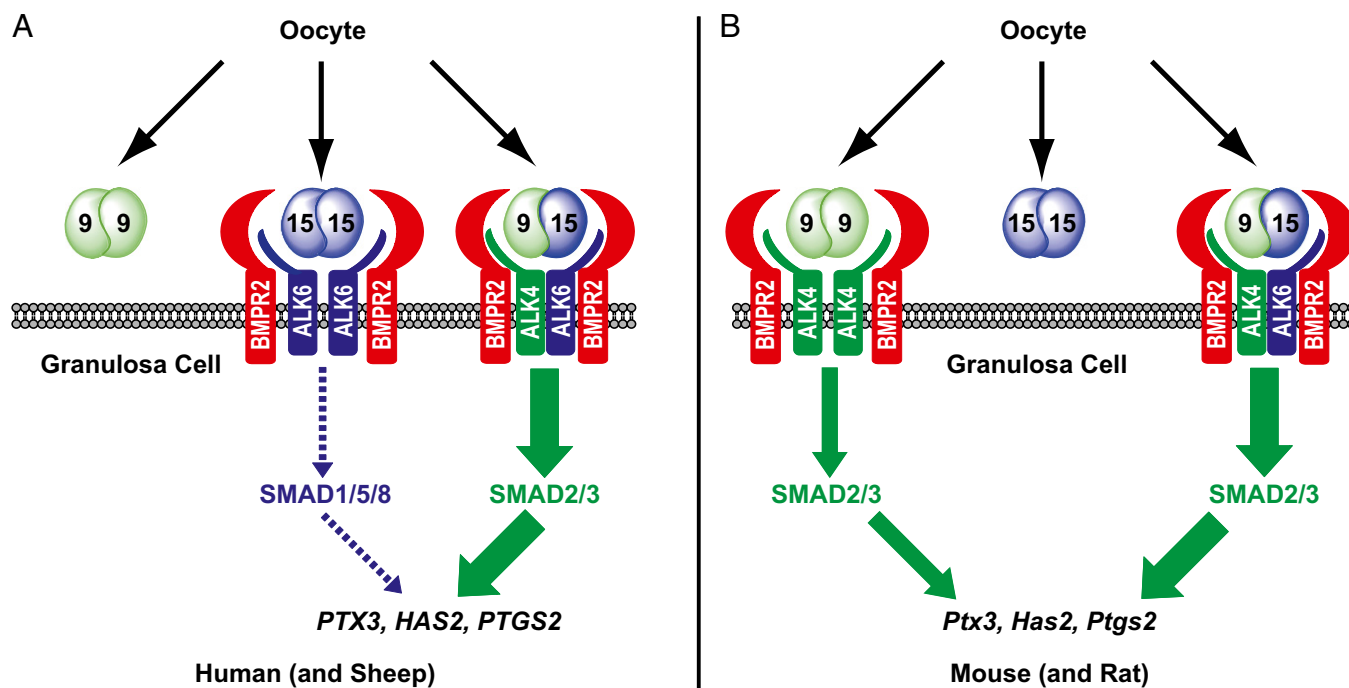
www.manaraa.com

Fig. 7. Models for BMP15 and GDF9 homodimers and GDF9:BMP15 heterodimers in regulating cumulus granulosa cell functions. (*A*) In human (and sheep), the GDF9:GDF9 homodimer has extremely low activity. Active BMP15:BMP15 homodimer binds to BMPR2 and ALK6 to up-regulate ECM genes minimally via a SMAD1/5/8 pathway, whereas the potent GDF9:BMP15 heterodimer likely binds to a BMPR2-ALK4-ALK6 receptor complex to transmit a signal through phosphorylation of SMAD2/3. (*B*) In mouse (and rat), BMP15:BMP15 is inactive, whereas the GDF9:GDF9 homodimer cooperates with the GDF9:BMP15 heterodimer to regulate granulosa cell function via a SMAD2/3 pathway starting from secondary follicles. The GDF9:GDF9 homodimer is likely the dominant (active) ligand in primary follicles.

Our data also have important implications for human oocyte in vitro maturation (IVM), an infertility treatment modification of traditional in vitro fertilization protocols (43). The objectives of IVM in human assisted reproductive technology (ART) are to avoid side effects of exogenous gonadotropins, to increase fetal viability, and to reduce the cost of infertility treatments. High expression of cumulus expansion-regulated genes (e.g., *PTGS2*, *HAS2*) is correlated with high-quality embryos in the ART clinic (44–46), and we have shown that GDF9:BMP15 heterodimers are the most bioactive ligands to up-regulate these ECM genes in vitro. However, because oocyte developmental competence is enhanced by oocyte-derived paracrine factors during IVM (47), GDF9:BMP15 heterodimers are potential ligands for promoting oocyte developmental competence in vitro during IVM and provide new opportunities for treatment of human infertility.

Materials and Methods

Construction of Expression Plasmids. Plasmids containing the native h/mGDF9 and h/mBMP15 cDNA were used as templates, and overlap extension PCR was performed to engineer optimized cleavage sites and FLAG- or MYC-tag sequences before the ligand mature domains as well as to fuse the pre-propeptide and modified mature domains (6). To enhance the expression of mGDF9/BMP15 in HEK-293T cells, the mature mouse prepro domain was replaced by the human prepro domain (Fig. S1*A*). For homodimer expression plasmids, FLAG-tagged h/mGDF9 or h/mBMP15 sequences were cloned into pEFIRES-P. For heterodimer expression plasmids, both MYC-tagged h/mGDF9 and FLAG-tagged h/mBMP15 were cloned into pCEBud4.1 (Invitrogen). MYC-h/mGDF9 is under the control of the EF-1α promoter, whereas FLAG-h/mBMP15 is under the control of the CMV promoter in pCEBud4.1. The cDNAs encoding the engineered precursor sequences in the expression plasmids were confirmed by DNA sequencing.

Transfection and Selection of Stable Cell Clones. HEK-293T cells were obtained from the tissue culture core at Baylor College of Medicine and cultured in DMEM containing 10% (vol/vol) FBS and 100 μg/mL penicillin–streptomycin.

All plasmids were transfected into HEK-293T cells using FuGENE6 (Roche) transfection reagent according to the manufacturer's instructions. Two days after transfection, cells containing the homodimer expression plasmids (pEFIRES-P) were selected with 5 μg/mL of puromycin (Invitrogen), and cells containing the heterodimer expression plasmids (pCEBud4.1) were selected under 500 μg/mL of Zeocin (Invitrogen). Puromycin/Zeocin-resistant cell colonies were selected 2 wk after transfection, and protein expression was confirmed by Western blot. HEK-293 hBMP15 stable cell lines were generated as described in our previous study (6).

Protein Purification, Quantification, and Immunoprecipitation. When stable cells reached confluency, DMEM containing 2% (vol/vol) FBS and 100 μg/mL penicillin–streptomycin was used for the production of recombinant proteins. Roller-bottle cultures were harvested 5 d after seeding, and dishes were harvested 3 d after seeding. Purification of FLAG-tagged homodimers was conducted using anti-FLAG M2 affinity gel (Sigma-Aldrich) according to the manufacturer's protocol. The FLAG-tagged homodimers were eluted with 3× FLAG elution buffer (25 μg/μL in Tris-buffered saline, pH8.0), and 1 mg/mL BSA was added to the proteins before storage at −80 °C. The purified FLAG-tagged ligands were quantified by Western blot using FLAG-bacterial alkaline phosphatase standards and mouse anti-FLAG M2 antibody (Sigma-Aldrich) (Fig. S1*B*, *Left*). MYC-GDF9:FLAG-BMP15 heterodimers were immunoprecipitated by the same method as above. The purified MYC-m/hGDF9 was quantified using FLAG-mGDF9 standards with a GDF9 monoclonal antibody as described in our previous study (22) (Fig. S1*B*, *Right*).

Mouse Granulosa Cell Isolation. Mice used in this study were maintained on a mixed C57BL/6/129S6/SvEv genetic background and handled according to the National Institutes of Health *Guide for the Care and Use of Laboratory Animals* (48). Female mice 21–24 d of age were injected with 5 IU pregnant mare's serum gonadotropin, and ovaries were harvested 44–46 h after injection. Mouse granulosa cells were released by puncturing large antral follicles. The collection medium was DMEM/F12 containing 0.3% BSA, 100 μg/mL penicillin–streptomycin, and 10 mM Hepes. To remove oocytes, the cell suspension was filtered through a 40-μm nylon cell strainer and washed twice with collection medium.

Mouse and Human Granulosa Cell Assays. Mouse granulosa cells and COV434 cells were maintained in DMEM/F12 containing insulin-transferrin-sodium selenite supplement (Sigma-Aldrich), 0.5% heat-inactivated FBS, and 100 μg/mL penicillin–streptomycin. In the gene-induction assays, mouse granulosa cells were treated with ligands for 5 h, and total RNA was extracted. Real-time PCR was conducted to test the fold changes of *Ptx3*, *Has2*, and *Ptgs2*. For SMAD activation analysis, mouse granulosa cells and COV434 cells were treated with ligands for 1 h and lysed with RIPA buffer in the presence of proteinase and phosphatase inhibitors (Roche). SMAD phosphorylation was detected by Western blot with anti–P-SMAD1/5/8 or anti–P-SMAD2/3 (Cell Signaling). Actin was used as the internal control detected by monoclonal anti-actin (Sigma-Aldrich).

Mouse Cumulus Expansion Assay. In vitro mouse cumulus expansion assays were performed as described previously (49). Briefly, oocytes were removed from oocyte-cumulus cell complexes using a microsurgical apparatus. The resulting OOX complexes consisted of the spherical zona pellucida surrounded by the cumulus cell mass without the oocyte. The culture medium used in the assay was Eagle's minimal essential medium (MEM) alpha medium containing 5% (vol/vol) FBS and 10 mM milrinone (Sigma-Aldrich). Ten OOX cumulus cells were treated with ligands in the presence of 10 ng/mL EGF. After 15 h incubation, the cumulus expansion index was scored based on the degree of OOX cumulus cell expansion using a scale from 0 (no expansion) to 4 (complete expansion) (49).

Receptor Selectivity Assay. Mouse granulosa cells or COV434 cells were treated with ligand and coincubated with/without 100 nM LDN-193189, 1 μM SB-505124, or 1 μg BMPR2, ACVR2A, ACVR2B, or TGFBR2 ECD with an Ig Fc tag (R&D). For BMPR2* (made in the laboratory of T.B.T), the ECD of hBMPR2 (amino acids 27-150) was cloned into the pFUSE-Fc vector (Invivogen). Recombinant hBMPR2-Fc fusion protein was generated by transient expression in HEK-293 Freestyle cells and purified by affinity chromatography using protein G affinity resin.

Real-Time PCR. Gene expression was analyzed by real-time PCR using the 7500 Fast Real-time System (Applied Biosystems). Taqman gene-expression probes (*Ptx3* Mm00477267_g1, *Has2* Mm00515089_m1, and *Ptgs2* mM00478374_m1) were used to test the fold changes of the three transcripts. All real-time PCR analyses were performed in duplicate, and the results were reported from at least three independent experiments. The relative fold change of transcript was calculated by the $2^{-\Delta\Delta CT}$ method as described previously (50) and was normalized to *Gapdh* as an endogenous reference.

Statistical Analysis. All experiments presented in this study were repeated at least three times independently. Differences among groups were analyzed for statistical significance by using one-way ANOVA followed by Tukey's multiple comparison test. Comparison of means between two groups was made by Student *t* test. The data represent the mean ± SEM, and $P < 0.05$ was considered to be statistically significant.

1. Chang H, Brown CW, Matzuk MM (2002) Genetic analysis of the mammalian TGF-β superfamily. *Endocr Rev* 23:787–823.
2. Matzuk MM, Burns KH (2012) Genetics of mammalian reproduction: Modeling the end of the germline. *Annu Rev Physiol* 74:503–528.
3. Otsuka F, McTavish KJ, Shimasaki S (2011) Integral role of GDF-9 and BMP-15 in ovarian function. *Mol Reprod Dev* 78(1):9–21.
4. Mazerbourg S, et al. (2004) Growth differentiation factor-9 signaling is mediated by the type I receptor, activin receptor-like kinase 5. *Mol Endocrinol* 18(3):653–665.
5. Moore RK, Otsuka F, Shimasaki S (2003) Molecular basis of bone morphogenetic protein-15 signaling in granulosa cells. *J Biol Chem* 278(1):304–310.
6. Li Q, Rajanahally S, Edson MA, Matzuk MM (2009) Stable expression and characterization of N-terminal tagged recombinant human bone morphogenetic protein 15. *Mol Hum Reprod* 15(12):779–788.
7. Dong J, et al. (1996) Growth differentiation factor-9 is required during early ovarian folliculogenesis. *Nature* 383(6600):531–535.
8. Yan C, et al. (2001) Synergistic roles of bone morphogenetic protein 15 and growth differentiation factor 9 in ovarian function. *Mol Endocrinol* 15(6):854–866.
9. Su YQ, et al. (2004) Synergistic roles of BMP15 and GDF9 in the development and function of the oocyte-cumulus cell complex in mice: Genetic evidence for an oocyte-granulosa cell regulatory loop. *Dev Biol* 276(1):64–73.
10. Hanrahan JP, et al. (2004) Mutations in the genes for oocyte-derived growth factors GDF9 and BMP15 are associated with both increased ovulation rate and sterility in Cambridge and Belclare sheep (Ovis aries). *Biol Reprod* 70(4):900–909.
11. Galloway SM, et al. (2000) Mutations in an oocyte-derived growth factor gene (BMP15) cause increased ovulation rate and infertility in a dosage-sensitive manner. *Nat Genet* 25(3):279–283.
12. Dixit H, et al. (2006) Missense mutations in the BMP15 gene are associated with ovarian failure. *Hum Genet* 119(4):408–415.
13. Laissue P, et al. (2006) Mutations and sequence variants in GDF9 and BMP15 in patients with premature ovarian failure. *Eur J Endocrinol* 154(5):739–744.
14. Hoekstra C, et al. (2008) Dizygotic twinning. *Hum Reprod Update* 14(1):37–47.
15. Liao WX, Moore RK, Otsuka F, Shimasaki S (2003) Effect of intracellular interactions on the processing and secretion of bone morphogenetic protein-15 (BMP-15) and growth and differentiation factor-9. Implication of the aberrant ovarian phenotype of BMP-15 mutant sheep. *J Biol Chem* 278(6):3713–3719.
16. McNatty KP, et al. (2005) Bone morphogenetic protein 15 and growth differentiation factor 9 co-operate to regulate granulosa cell function in ruminants. *Reproduction* 129(4):481–487.
17. Reader KL, et al. (2011) Signalling pathways involved in the cooperative effects of ovine and murine GDF9+BMP15-stimulated thymidine uptake by rat granulosa cells. *Reproduction* 142(1):123–131.
18. Mottershead DG, Ritter LJ, Gilchrist RB (2012) Signalling pathways mediating specific synergistic interactions between GDF9 and BMP15. *Mol Hum Reprod* 18(3):121–128.
19. Eppig JJ (1979) Gonadotropin stimulation of the expansion of cumulus oophori isolated from mice: General conditions for expansion in vitro. *J Exp Zool* 208(1):111–120.
20. Matzuk MM, Burns KH, Viveiros MM, Eppig JJ (2002) Intercellular communication in the mammalian ovary: Oocytes carry the conversation. *Science* 296(5576):2178–2180.
21. Chen L, Russell PT, Larsen WJ (1993) Functional significance of cumulus expansion in the mouse: Roles for the preovulatory synthesis of hyaluronic acid within the cumulus mass. *Mol Reprod Dev* 34(1):87–93.
22. Elvin JA, Clark AT, Wang P, Wolfman NM, Matzuk MM (1999) Paracrine actions of growth differentiation factor-9 in the mammalian ovary. *Mol Endocrinol* 13(6):1035–1048.
23. Varani S, et al. (2002) Knockout of pentraxin 3, a downstream target of growth differentiation factor-9, causes female subfertility. *Mol Endocrinol* 16(6):1154–1167.
24. Lim H, et al. (1997) Multiple female reproductive failures in cyclooxygenase 2-deficient mice. *Cell* 91(2):197–208.
25. Elvin JA, Yan C, Matzuk MM (2000) Growth differentiation factor-9 stimulates progesterone synthesis in granulosa cells via a prostaglandin E2/EP2 receptor pathway. *Proc Natl Acad Sci USA* 97(18):10288–10293.
26. Buccione R, Vanderhyden BC, Caron PJ, Eppig JJ (1990) FSH-induced expansion of the mouse cumulus oophorus in vitro is dependent upon a specific factor(s) secreted by the oocyte. *Dev Biol* 138(1):16–25.
27. Li Q, et al. (2008) Redundant roles of SMAD2 and SMAD3 in ovarian granulosa cells in vivo. *Mol Cell Biol* 28(23):7001–7011.
28. Pangas SA, et al. (2008) Conditional deletion of Smad1 and Smad5 in somatic cells of male and female gonads leads to metastatic tumor development in mice. *Mol Cell Biol* 28(1):248–257.
29. Yi SE, et al. (2001) The type I BMP receptor BmprIB is essential for female reproductive function. *Proc Natl Acad Sci USA* 98(14):7994–7999.
30. Cuny GD, et al. (2008) Structure-activity relationship study of bone morphogenetic protein (BMP) signaling inhibitors. *Bioorg Med Chem Lett* 18(15):4388–4392.
31. Yu PB, et al. (2008) BMP type I receptor inhibition reduces heterotopic [corrected] ossification. *Nat Med* 14(12):1363–1369.
32. DaCosta Byfield S, Major C, Laping NJ, Roberts AB (2004) SB-505124 is a selective inhibitor of transforming growth factor-beta type I receptors ALK4, ALK5, and ALK7. *Mol Pharmacol* 65(3):744–752.
33. Vitt UA, Mazerbourg S, Klein C, Hsueh AJ (2002) Bone morphogenetic protein receptor type II is a receptor for growth differentiation factor-9. *Biol Reprod* 67(2):473–480.
34. Mathews LS, Vale WW (1991) Expression cloning of an activin receptor, a predicted transmembrane serine kinase. *Cell* 65(6):973–982.
35. Israel DI, et al. (1996) Heterodimeric bone morphogenetic proteins show enhanced activity in vitro and in vivo. *Growth Factors* 13(3-4):291–300.
36. Pulkki MM, et al. (2012) A covalently dimerized recombinant human bone morphogenetic protein-15 variant identifies bone morphogenetic protein receptor type 1B as a key cell surface receptor on ovarian granulosa cells. *Endocrinology* 153(3):1509–1518.
37. Li Q, et al. (2011) Transforming growth factor β receptor type 1 is essential for female reproductive tract integrity and function. *PLoS Genet* 7(10):e1002320.
38. Carlsson LM, et al. (2009) ALK7 expression is specific for adipose tissue, reduced in obesity and correlates to factors implicated in metabolic disease. *Biochem Biophys Res Commun* 382(2):309–314.
39. Guo J, Wu G (2012) The signaling and functions of heterodimeric bone morphogenetic proteins. *Cytokine Growth Factor Rev* 23(1-2):61–67.

40. Hayashi M, et al. (1999) Recombinant growth differentiation factor-9 (GDF-9) enhances growth and differentiation of cultured early ovarian follicles. *Endocrinology* 140(3):1236–1244.

41. Elvin JA, Yan C, Matzuk MM (2000) Oocyte-expressed TGF-beta superfamily members in female fertility. *Mol Cell Endocrinol* 159(1-2):1–5.

42. Erickson GF, Shimasaki S (2003) The spatiotemporal expression pattern of the bone morphogenetic protein family in rat ovary cell types during the estrous cycle. *Reprod Biol Endocrinol* 1:9.

43. Smitz JE, Thompson JG, Gilchrist RB (2011) The promise of in vitro maturation in assisted reproduction and fertility preservation. *Semin Reprod Med* 29(1):24–37.

44. McKenzie LJ, et al. (2004) Human cumulus granulosa cell gene expression: A predictor of fertilization and embryo selection in women undergoing IVF. *Hum Reprod* 19(12): 2869–2874.

45. Cillo F, et al. (2007) Association between human oocyte developmental competence and expression levels of some cumulus genes. *Reproduction* 134(5):645–650.

46. Anderson RA, et al. (2009) Cumulus gene expression as a predictor of human oocyte fertilisation, embryo development and competence to establish a pregnancy. *Reproduction* 138(4):629–637.

47. Hussein TS, Thompson JG, Gilchrist RB (2006) Oocyte-secreted factors enhance oocyte developmental competence. *Dev Biol* 296(2):514–521.

48. Committee for the Update of the Guide for the Care and Use of Laboratory Animals (2011) *Guide for the Care and Use of Laboratory Animals* (National Academies Press, Washington, DC), 8th Ed.

49. Vanderhyden BC, Caron PJ, Buccione R, Eppig JJ (1990) Developmental pattern of the secretion of cumulus expansion-enabling factor by mouse oocytes and the role of oocytes in promoting granulosa cell differentiation. *Dev Biol* 140(2): 307–317.

50. Livak KJ, Schmittgen TD (2001) Analysis of relative gene expression data using real-time quantitative PCR and the 2(-Delta Delta C(T)) method. *Methods* 25(4): 402–408.

PHYSIOLOGY

Peng et al.

www.manaraa.com